Hydrogen/Hydrogen Exchange and Formation of Dihydrogen Derivatives of Rhenium Hydride Complexes in Acidic Solutions

Sibylle Feracin,[†] Tobias Bürgi,[†] Vladimir I. Bakhmutov,[†,‡] Igor Eremenko,[†]
Evgenii V. Vorontsov,[‡] Alexey B. Vimenits,[‡] and Heinz Berke[*,†]

Anorganisch-chemisches Institut der Universität Zürich, Winterthurerstrasse 190, 8057 Zürich, Switzerland, and Russian Academy of Sciences, A. N. Nesmeyanov Institute of Organo-Element Compounds, Vavilov Str. 28, Moscow 117 813, Russia

Received December 28, 1993[®]

Protonation of $Re(CO)H_2(NO)L_2$ complexes (L = $PiPr_3$ (**1a**), $P(OiPr)_3$ (**1b**), PMe_3 (**1c**)) with stoichiometric or excess amounts of CF_3COOH yields the monohydrido trifluoroacetato compounds $Re(CO)H(NO)L_2(OOCCF_3)$ (L = $PiPr_3$ (**3a**), $P(OiPr)_3$ (**3b**), PMe_3 (**3c**)) and bis(trifluoroacetato) complexes $Re(CO)(NO)L_2(OOCCF_3)_2$ (L = $PiPr_3$ (**4a**), $P(OiPr)_3$ (**4b**), PMe_3 (**4c**)). **3c** has been characterized by single-crystal X-ray diffraction, confirming a trans NO, H configuration: space group $P2_1/n$, $a = 10.290(2)$, $b = 11.454(3)$, $c = 15.232(4)$ Å; $\beta = 101.01(2)°$; $V = 176.2(7)$ Å^3; $\varrho_{calcd} = 1.924$ g/cm^3; $R = 0.043$, $R_w = 0.079$. The interaction of $Re(CO)H_2(NO)L_2$ (**1**) and of *cis*-$ReH(CO)(PMe_3)_4$ (**5**) with acidic compounds (CF_3COOH, $HBF_4{\cdot}Et_2O$, and $[(3,5\text{-}(CF_3)_2C_6H_3)_4B]^-[H(OEt_2)_2]^+$) was investigated by detailed NMR studies. For the diastereomeric Re hydride sites the kinetics of the fast H(hydride)/H(acid) exchanges (trans to NO) and of the slower formation of the cationic dihydrogen complexes **2** (preferably trans to CO) accompanied by dihydrogen elimination were determined. In the presence of CF_3COOH **2a** rapidly reduces benzaldehyde to benzyl alcohol.

Introduction

Hydrogen/deuterium exchange with D acids and D alcohols is well documented for many acidic terminal hydrides, such as $HCo(CO)_4$ and $HMn(CO)_5$.[1a,b] For hydridic transition-metal hydrides, on the other hand,[1c,d] this is a rare process, since elimination of dihydrogen rather than H/D exchange can occur in the course of these isotopomerization reactions. Although dihydrogen complexes have been suggested as transients of the H_2 elimination, nonclassical hydride species could not be detected in most cases.[2] A very recent example of an intramolecular H/D exchange has been reported by Morris et al.[2c] for $[IrH_2(DS(CH_2)_3SD)(PCy_3)_2][BF_4]$, which also quite likely proceeds through a nonobservable (HD) complex. Herein, we report on NMR studies of acidic solutions of some Re hydride complexes, which undergo facile H/D exchange with half-life times in the range of the NMR time scale. In addition, protonation of these complexes gives the detectable nonclassical dihydrogen complexes, which suffer from further H_2 elimination.

Results and Discussion

Preparative Results and Structure Determination of 3c. $ReH_2(CO)(NO)L_2$ complexes (L = $PiPr_3$, **1a**; L = $P(OiPr)_3$, **1b**; L = PMe_3, **1c**) react at room temperature with 1 equiv of CF_3COOH in CH_2Cl_2 to yield selectively the corresponding trifluoroacetato monohydrido complexes **3a–c**, with the H and the CO ligands in cis positions (eq 1). In the presence of excess acid, a further 1 equiv of H_2 is eliminated at temperatures above −40 °C, and compounds **4a–c** are formed in high yields. Both protonation steps are presumed to proceed via the intermediacy of the unstable nonclassical dihydrogen species $[Re(H_2)H(CO)(NO)L_2]^+$ (L = $PiPr_3$, **2a**; L = $P(OiPr)_3$, **2b**; L = PMe_3, **2c**) and $[Re(H_2)(OC(O)CF_3)(CO)(NO)L_2]^+$ complexes, respectively.

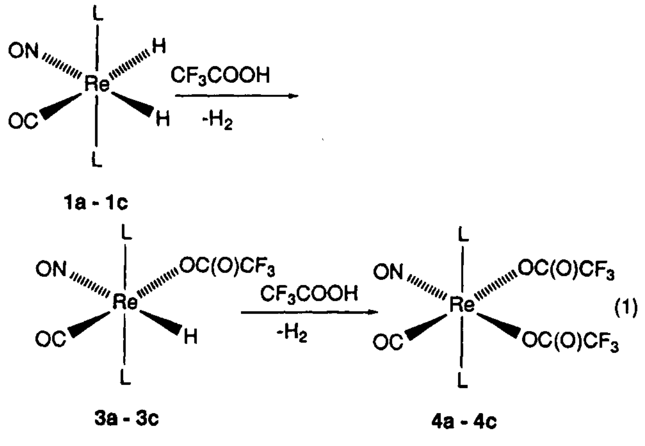

L = $PiPr_3$ (**a**), $P(OiPr)_3$ (**b**), PMe_3 (**c**)

The X-ray crystal structure of complex **3c** established the trans positions of the CO and the trifluoroacetato ligands (Figure 1 and Table 1). The trans PReP unit in complex **3c** (Re–P = 2.409(3) and 2.433(2) Å, P–Re–P = 163.2(1)°) is essentially orthogonal to the plane

---

[†] Universität Zürich.

[‡] A. N. Nesmeyanov Institute of Organo-Element Compounds.

[®] Abstract published in *Advance ACS Abstracts*, September 1, 1994.

(1) (a) Braterman, P. S.; Harrill, R. W.; Kaesz, H. D. *J. Am. Chem. Soc.* **1967,** *89,* 2851. (b) Ungvary, F.; Marko, L. *Organometallics* **1983,** *2,* 1608. (c) Gaus, P. L.; Kao, S. C.; Darensbourg, M. Y.; Arndt, L. W. *J. Am. Chem. Soc.* **1984,** *106,* 4752. (d) Van der Zeijden, A. A. H.; Sontag, C.; Bosch, H. W.; Shklover, V.; Berke, H.; Nanz, D.; Von Philipsborn, W. *Helv. Chim. Acta* **1991,** *74,* 1194. Bakhmotov, V. I.; Bürgi, T.; Berke, H. *Organometallics,* submitted for publication.

(2) (a) Jessop, P. G.; Morris, R. H. *Coord. Chem. Rev.* **1992,** *121,* 155. Heinekey, D. M.; Oldham, W. J., Jr. *Chem. Rev.* **1993,** *93,* 913. (b) Baker, M. V.; Field, L. D.; Young, D. J. *J. Chem. Soc., Chem. Commun.* **1988,** 546. (c) Jessop, P. G.; Morris, R. H. *Inorg. Chem.* **1993,** *32,* 2236.

0276-7333/94/2313-4194$04.50/0

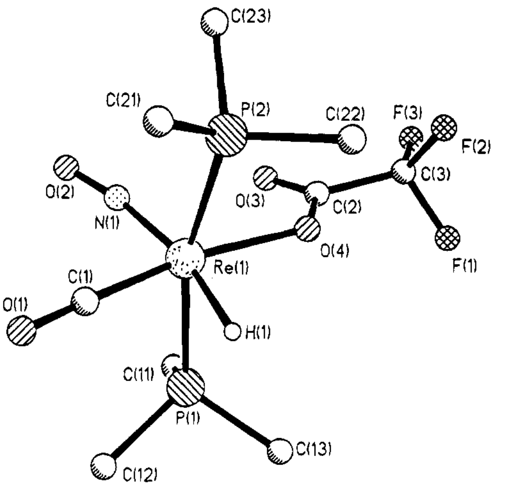

Figure 1. Molecular structure of **3c**.

Table 1. Selected Bond Lengths (Å) and Angles (deg) for 3c

Re(1)—P(1)	2.409(3)	Re(1)—P(2)	2.433(2)
Re(1)—O(4)	2.149(6)	Re(1)—N(1)	1.813(7)
Re(1)—C(1)	1.910(9)	Re(1)—H(1)	1.67(3)
O(1)—C(1)	1.122(13)	O(1)—N(1)	1.177(10)
O(3)—C(2)	1.167(12)	O(4)—C(2)	1.168(11)
P(1)—Re(1)—P(1)	163.2(1)	P(1)—Re(1)—P(4)	87.7(2)
P(2)—Re(1)—P(4)	83.0(2)	P(1)—Re(1)—N(1)	96.6(2)
P(2)—Re(1)—N(1)	98.7(2)	O(4)—Re(1)—P(1)	100.4(3)
P(1)—Re(1)—C(1)	91.9(3)	P(2)—Re(1)—C(1)	93.9(3)
O(4)—Re(1)—C(1)	166.4(3)	N(1)—Re(1)—C(1)	93.2(3)
O(4)—Re(1)—H(1)	92(2)	N(1)—Re(1)—H(1)	167(2)
C(1)—Re(1)—H(1)	75(2)		

spanned by the Re(I) atom, the oxygen atom of the trifluoroacetate group (Re—O = 2.149(6) Å), the CO group (Re—C = 1.910(9) Å, C—O = 1.122(13) Å), the NO ligand (Re—N = 1.813(7) Å, N—O = 1.177(10) Å), and the hydride atom (Re—H = 1.67(3) Å). Albeit having a high standard deviation, the Re—H bond length is close to the Re—H bond distance determined in a neutron diffraction study for a related Re complex.[3] The hydride and the NO ligand are oriented in trans positions, which has also been observed for quite a number of Re(CO)(NO)H(X)L_2 compounds.[4] Note that this is of particular interest for the structure of the dihydrogen complexes **2**, since the interconversion of **2** to **3** is a substitutional process at a d^6-configurated octahedral metal center, which normally proceeds with retention of configuration. Hence, the observed trans NO, H arrangement in complex **3c** suggests that the nonclassical dihydrogen complexes **2** will have the H_2 ligand trans to the CO group.

The NMR and IR data for **3a,b** are very similar to those of the structurally characterized compound **3c** and indicate that these complexes have comparable coordination geometries around the Re center. Evidence for the cis location of the H and CO ligands is provided by the $^2J_{H^{13}CO}$ coupling constants of 8.9, 10.2, and 9.9 Hz for **3a–c** obtained from proton-coupled ^{13}C NMR spectra.

NMR Characterization of the Nonclassical (H_2) Complexes 2. The protonation reaction of **1a**, affording **3a**, was the subject of a detailed NMR study. As reported in a previous paper,[5] protonation of **1a** with a 4-fold excess of CF_3COOH in CD_2Cl_2 at −90 °C gives the nonclassical (H_2) complex **2a**. At first glance, seemingly in contrast to the isolated sole final product **3a** (eq 1), ^1H NMR signals for a mixture of two isomers of nonclassical dihydrogen complexes are observed. These are formed in unequal amounts and interconvert on the NMR time scale. The major isomer, **2a**, is significantly more stable,[5] and in accord with our EHT model calculations (vide infra), we propose the structure shown in eq 1 for this species. Loss of H_2 from **2a** occurs above −70 °C (or D_2 from the corresponding $ReD(D_2)$ complex obtained from $\mathbf{1a}^{\mathbf{D}}$ and CF_3COOD), and the reaction rapidly goes to completion at −50 °C, yielding the final product **3a**. Since the ^1H NMR spectrum of the reaction mixture at −50 °C displayed a very sharp singlet for the extruded (free) H_2 at 4.55 ppm, and the overall features of the signals of **2a** were also essentially unchanged from spectra recorded at −90 °C, it is deemed that the ligand substitution of the metal-bound dihydrogen ligand by the CF_3COO^- group is *irreversible*.

Similarly, compound **1c** can be protonated with a 4-fold excess of CF_3COOH (−83 °C) to generate the new unstable cationic (H_2) complex **2c**. The ^1H NMR spectrum shows a broadened signal at −1.83 ppm for the hydrogen ligands with a T_1 time of 9.3 ms (200 MHz). At −100 °C, this signal is changed to a triplet resonances for the hydride ligand (−1.94 ppm, $J(H-P)$ = 27 Hz, T_1 = 8.5 ms) and to a very broad resonance for the (H_2) moiety (−1.6 to −1.7 ppm), thus demonstrating H/H_2 exchange on the NMR time scale.

In contrast to complexes **1a,c**, protonation of **1b** could only be accomplished with the stronger acid $HBF_3 \cdot 2Et_2O$ (at −90 °C). The resulting (H_2) complex **2b** gives rise to a signal at −1.9 ppm, which converts to a triplet for the hydride substituent (−2.18 ppm, $^2H_{PH}$ = 26 Hz) and to a very broad signal for the (H_2) moiety (−1.7 ppm) at −100 °C. The T_1(min) value for the averaged signals of the H and H_2 groups was found to be 4.9 ms (200 MHz, 190−195 K). This value resembles closely that of **2a**, for which T_1(min) = 7 ms (300 MHz) has been determined earlier.[5]

Unfortunately, the data given do not allow definite conclusions about the geometries of the H ligands at the metal centers in **2b,c**. The low-temperature NMR spectra of **2b,c** did, however, display resonances for just one isomer for both complexes. On the basis of our EHT calculations (vide infra), we propose that the (H_2) and the CO ligands in **2b,c** are, by analogy to the major isomer obtained for **2a**, also arranged in trans positions.

Kinetic Results. Detailed NMR investigations of the reaction of **1a** with varying amounts of CF_3COOH provided further insight into the protonation reactions. When **1a**/$CF_3COOH(D)$ ratios ≥1 were applied, signals for the parent hydride **1a** (or $\mathbf{1a}^{\mathbf{D}}$), as well as for the cationic complex **2a** (or $\mathbf{2a}^{\mathbf{D}}$), were detected in the ^1H (^2H) and $^{31}P\{^1H\}$ NMR spectra. Temperature-dependent NMR spectra between −95 and −70 °C established the protonation equilibrium shown in eq 2. The observed rates were found to be comparable to the NMR time scale.

---

[3] (a) Cotton, F. A.; Luck, R. L. *Inorg. Chem.* **1985**, *28*, 2182. (b) Emge, T. J.; Koetzle, T. F.; Bruno, J. W.; Caulton, K. G. *Inorg. Chem.* **1984**, *23*, 4012. (c) Abrachams, S. C.; Ginsburg, A. P.; Knox, K. *Inorg. Chem.* **1964**, *3*, 558.

[4] Hund, H.-U.; Ruppli, U.; Berke, H. *Helv. Chim. Acta* **1993**, *76*, 963.

[5] Gusev, D. G.; Nietlispach, D.; Eremenko, I. L.; Berke, H. *Inorg. Chem.* **1993**, *32*, 3628.

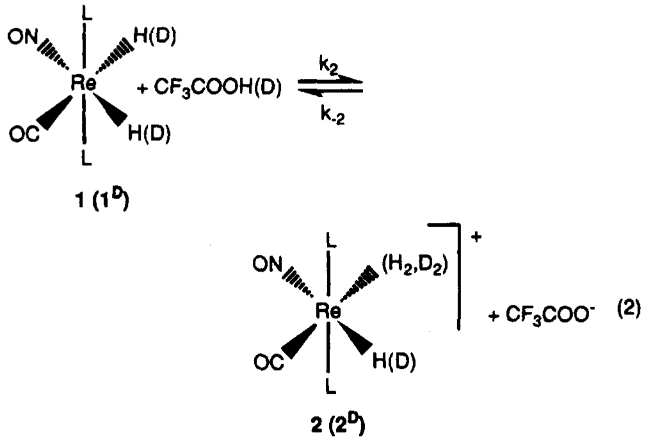

1 (**1**^{D})

2 (**2**^{D})

L = PiPr$_3$ (**a**), P(OiPr)$_3$ (**b**), PMe$_3$ (**c**)

The kinetic parameters for this reaction of **1a** (Table 2) were obtained from DNMR4[6] simulations of the $^{31}\{^1H\}$ NMR spectra. The kinetic order in CF_3COOH was found to be between 1.1 and 1.3, and the overall order of the reaction is approximately 2. The activation parameters are relatively high, and it appears quite unusual that a second-order reaction is accompanied by a positive $\Delta S^{\ddagger}$ value. The kinetic isotope effect, KIE, determined from the $^{31}P\{^1H\}$ NMR spectra of the protonations of **1a** and **1a**^{D} with CF_3COOH and CF_3COOD, respectively, is 1.4 ($k_2(H)/k_2(D) = 1.4$ at −80 °C.[9] Since the observed KIE is deemed significantly too small for such a process and the activation parameters are also quite unexpected, care should be taken to interpret these results in terms of just *one* elementary step. Therefore, it seems likely that the mechanism of the protonation reaction is rather complicated and has to be considered as a sequence of several steps which all contribute to the observed kinetic parameters. It should be noted that similar kinetic parameters have been determined for the protonation reaction of *cis*-ReD(CO)(PMe$_3$)$_4$ (**5**) with CF_3COOD in CD_2Cl_2. The NMR parameters of this complex and the cationic product [Re(D$_2$)(CO)(PMe$_3$)$_4$]$^+$ (**6**)[5,7] are also given in Table 2. The protonation reaction of **1c**, producing **2c**, is also second order but is considerably faster than that of **1a**. Since the electronic structures for both phosphine-substituted rhenium complexes are deemed very similar, the difference in reactivity presumably has to be attributed to the smaller steric hindrance in the PMe$_3$-substituted complex **1c**.

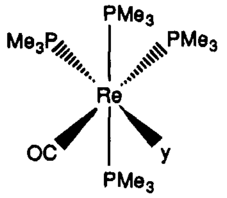

Y
D **5**
D$_2$]$^+$ **6**

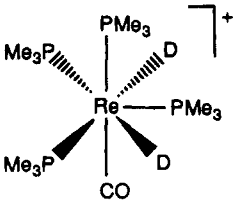

7

When the molar ratio **1a**/CF_3COOH was raised to 4 in the protonation reaction of **1a**, the $^{31}P\{^1H\}$ NMR spectra no longer exhibited signals for **2a**. Both H ligand resonances of **1a** were equally broadened in variable-temperature ^1H NMR experiments, and saturation of the CF_3COOH line at −75 °C resulted in magnetization transfer to both H ligand signals of **1a**. According to eqs 3 and 4,this could in principle correspond to competitive H/H exchanges of either of the two diastereotopic H positions. In this case the exchange rates of both H positions of **1a** would be expected to be about equal. However, it seems more reasonable to interpret this result in terms of a positional exchange of the H ligands via formation of the nonclassical dihydrogen complex **2a** (cf. eq 2). This would require a very fast intramolecular exchange between the H_2 and H ligands in **2a**.[5] For the formal exchange processes of eqs 3 and 4, rate constants k_3 and k_4 (15 × 10^2 L/(mol s)) were estimated from the line widths of the H ligand signals at −70 °C. A similar range of rate constants ((17−20) × 10^2 L/(mol s)) was obtained from $^{31}P\{^1H\}$ NMR kinetic measurements for the same reaction when higher concentrations of the acid were applied (**1a**/CF_3COOH < 4), i.e. in the regime where the signals of the nonclassical dihydrogen complex **2a** are still detectable.

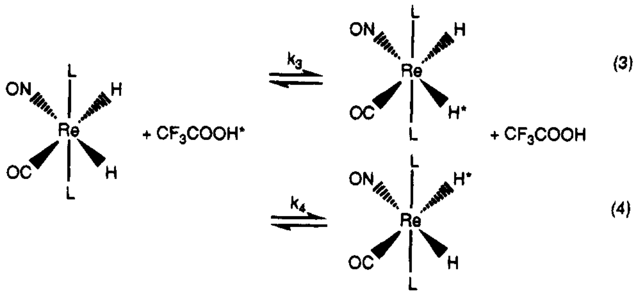

The protonation reactions of the coordinatively saturated complexes **1**, yielding **2** (eq 2), are rapid and reversible on the NMR time scale. The substitution of the H_2 moiety in **2**, which gives the final trifluoroacetato products **3**, on the other hand, is a slower, irreversible process (vide supra). It should be noted at this point that the formation of *classical* cationic trihydride complexes might be considered as an alternative pathway for the observed protonation processes. Two pieces of evidence, however, provide strong arguments against the required direct proton attack at the metal center. (a) Even at −120 °C, signals for a trihydride complex have not been observed in the NMR spectra of acidic solutions of **1a**.[5] (b) Although one might argue that such a species is formed in a very low concentration and can hence not be detected, this would require that the acidity of the trihydride species is higher than that of the nonclassical isomer **2a**.[2a] Note, however, that this would contradict some reports, which manifest that dihydrogen complexes normally display a higher acidity than their classical dihydride congeners.[8] This general picture could also be confirmed in earlier studies on the protonation reaction of **5**, which showed that the nonclassical dideuterium complex **6** is indeed converted to the classical isomer [ReD$_2$(CO)(PMe$_3$)$_4$]$^+$ (**7**) above −30

---

[6] Bushweller, C. H.; Leterare, L. J.; Brunelle, J. A.; Bilofsky, H. S.; Whalon, M. R.; Fleischman, S. H. Quantum Chemistry Program Exchange, No. 466, DNMR-4.

[7] ^2H T_1 measurements were used to determine the kinetic parameters.[10]

[8] Chinn, M. S.; Heinekey, D. M. *J. Am. Chem. Soc.* **1990**, *112*, 5166.

[9] No pronounced kinetic isotope effect was observed for intramolecular H/D transfer between the thiol and hydride ligands in [IrH$_2$(DS(CH$_2$)$_3$SD)(PCy$_3$)$_2$][BF$_4$] at 22 °C in CD_2Cl_2.[2c]

Table 2. Kinetic Parameters of Protonations, Deprotonations (Eq 2), and Proton Exchanges (Eqs 3 and 4) Obtained from NMR Data for Re Hydride Complexes 1, 2a, 5, and 6

compd (eq), rate const	k, 10^2 L/(mol s) (t, °C)	E_a, kcal/mol	$\Delta H^{\ddagger}$ kcal/mol	$\Delta S^{\ddagger}$, eu	solvent
1a (2), k_2	4.4 (−80)	11.5 ± 0.5	11.1 ± 0.5	12.0 ± 2.5	CD_2Cl_2
1a^D (2), k_2	3.1 (−80)	10.4 ± 0.6	10.1 ± 0.6	5.8 ± 2.5	CH_2Cl_2
1a (3), k_3	33.7 (−70)	8.1 ± 0.2	7.7 ± 0.2	−2.3 ± 1.1	toluene-d_8
1a^D (3), k_3	16.0 (−70)				toluene
	6.5 (−80)				
1b (3, 4), k_3, k_4	20.7 (−66)	7.7 ± 0.6	7.4 ± 0.6	−5.5 ± 0.3	CD_2Cl_2
1b^D (3), k_3	3.6 (−70)	6.4 ± 0.3	6.0 ± 0.3	−16.6 ± 0.7	toluene/CH_2Cl_2 (1/1)
1b^D (4), k_4	0.93 (−60)	8.1 ± 0.4	7.7 ± 0.4	−13.9 ± 0.9	toluene/CH_2Cl_2 (1/1)
1b^D (3), k_3	4.6 (−70)	7.5 ± 0.3	7.1 ± 0.3	−10.3 ± 0.8	toluene
	2.2 (−80)				
1c (2), k_2	191.6 (−90)	13.9 ± 0.8	13.5 ± 0.8	36.8 ± 8	CD_2Cl_2
1c (3), k_3	252.2 (−73)	8.2 ± 0.2	7.8 ± 0.2	0 ± 3	toluene-d_8
2a (2), k_{-2}	76.8 (−80)	11.5 ± 0.5	11.1 ± 0.5	17.6 ± 3	CD_2Cl_2
2a^D (2), k_{-2}	32.1 (−80)	10.9 ± 0.5	9.6 ± 0.5	7.6 ± 2.0	CH_2Cl_2
5 (3), k_3[a]	0.92 (−60)	6.8 ± 0.2	6.3 ± 0.2	−19.2 ± 2.0	CH_2Cl_2
6 (2), k_2[a]	0.28 (−55)	14.8 ± 0.7	14.4 ± 0.7	14.8 ± 3.5	CH_2Cl_2

[a] Reaction steps analogous to eqs 2 and 3.

°C in CH_2Cl_2.[5] When a 1/1 ratio of **5**/CF_3COOD was used in the protonation reaction of **5**, the ^2H NMR spectrum displayed resonances of **5**–**7** simultaneously. While the D ligand signals of **5** and **6** coalesced at −35 °C, thus indicating exchange between these species, the ReD_2 resonance of the classical dihydride complex **7** remained sharp. From the latter observation it can be concluded that the nonclassical isomer **6** possesses a higher kinetic acidity than its classical hydride congener.[2a]

Changing the solvent in these protonation reactions, we observed drastic effects. When the less polar toluene was used in the reaction of **1a** with CF_3COOH or of **1a**^{D} with CF_3COOD, the dihydrogen complex **2a** or the $ReD(D_2)^+$ species **2a**^{D} turned out to be unstable and elimination of H_2 or D_2 was observed even at low temperatures between −90 and −70 °C. This is best exemplified for the reaction of CF_3COOH with **1a** (1/1 ratio) at −90 °C, which gave a mixture containing 55%, 7%, and 35% of **1a**, **2a**, and **3a**, respectively. Furthermore, inspection of the $^{31}P\{^1H\}$ NMR spectra of acidic solutions of **1a** below −70 °C showed that the protonation reaction according to eq 2 is considerably slowed down on the NMR time scale (Table 2).

In addition to these observations, the ^1H NMR spectrum of the protonations of **1a** with CF_3COOH in toluene revealed another quite surprising phenomenon: From −90 to −70 °C a dramatic *selective* line broadening of the signal for the H ligand located trans to the NO group was observed (Figure 2a). Saturation of the $^1H_{CF_3COOH}$ line at −75 °C led to exclusive polarization transfer to this particular resonance. Thus, even when the protonation according to eq 2 is slow, a quite fast H/H exchange process operates on the NMR time scale according to eq 3 (Table 2). The kinetic isotope effect for the exchange reaction of **1a** (eq 3) was found to be exceedingly higher than that for the protonation (eq 2): $k_3(H)/k_3(D) = 3.9$ versus $k_2(H)/k_2(D) = 1.4$ at −80 °C in CH_2Cl_2.[7]

Similarly, a regiospecific H/H exchange was also established for the protonation of **1b** with CF_3COOH (ratio 1.2) in toluene in low-temperature NMR studies (eq 3). ^2H NMR investigations of the ^2H isotopomers in toluene turned out to be especially suited for the observation of this exchange process (see Figure 2b). In contrast to the −70 °C spectrum, the room-temperature ^2H NMR spectrum revealed a strongly broadened signal for the D ligand located trans to the NO group (the CF_3COOD line is also broadened), while the resonance for the D ligand trans to CO is essentially unchanged from the low-temperature spectrum. It is worthy to note that the cationic dideuterium complex **2b**^{D} was not detected under these conditions and also, in a related issue, that the NMR spectra remained unchanged even when a 4-fold excess of acid was used. This demonstrates that the preference for the D/D (and H/H) exchange of the D and H ligands, respectively, trans to the NO group is

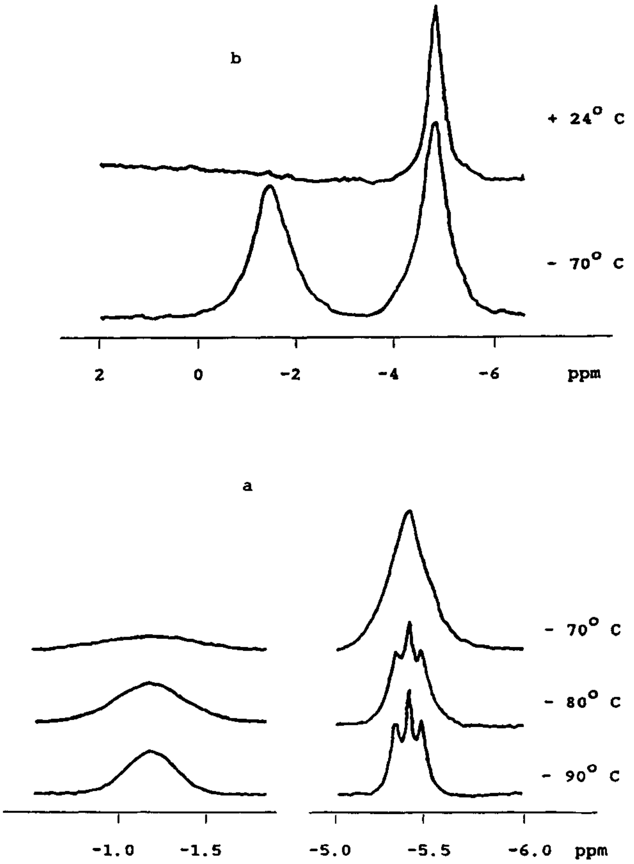

Figure 2. Temperature-dependent ^1H NMR spectra of **1a** (a) and ^2H NMR spectra of **1b** (b) in toluene or toluene-d_8 in the presence of CF_3COOH or CF_3COOD, displaying the rhenium hydride (a) and the rhenium deuteride chemical shift region (b).

particularly pronounced for the phosphite-substituted complex **1b**. We noticed, however, a reduced selectivity for this process when the solvent polarity was increased. This is best seen from the kinetic parameters for the protonation of $\mathbf{1b}^{\mathrm{D}}$, determined in neat CH_2Cl_2 and also in a 1/1 mixture of CH_2Cl_2 and toluene; a higher activation parameter, i.e. a slower exchange according to eq 3, was observed in a more polar solvent mixture (Table 2).[10] Equally evident, a reduced selectivity of this process in more polar solvents is also manifested in the ^1H NMR spectrum of a solution of **1b** and CF_3COOH (CF_3COOH/**1b** ratio 1.8) in CD_2Cl_2. The equal broadening of both signals of the diastereotopic H ligands in the temperature range 190–210 K clearly indicates that exchange according to both eqs 3 and 4 is operative (for kinetic parameters see Table 2).

A regioselective exchange according to eq 3 was also observed for complex **1c** in toluene (**1c**/CF_3COOH ratio 3) in the ^1H NMR spectra between 175 and 210 K (Table 2). Note that signals for the cationic complex **2c** were also not detectable under these conditions.

In further NMR studies we probed the influence of the acid strength and the acid counterion of the protonation and exchange equilibria of complexes **1**. Addition of the quite strong acid $[(3,5\text{-}(CF_3)_2C_6H_3)_4B]^-[H(OEt_2)]^+$ [11] to a CD_2Cl_2 solution of **1a** caused protonation with formation of **2a** according to eq 2. In this reaction the ^1H and ^{31}P NMR signals of **1a** and **2a** remained very sharp up to −65 °C, thus indicating retardation of eqs 2 and 3 on the NMR time scale. Even with the acid/**1a** ratio equal to 6, the equilibrium position of eq 2 remained on the left side (k_2/k_{-2} = 0.04 at −80 °C). Similar observations were made for the protonation of **1b**, which can only be achieved by addition of a large excess of $HBF_4 \cdot 2Et_2O$ in CD_2Cl_2.

Apparently, a strong acid seems to allow the H_2 ligand formation. It should be noted, however, that the thermodynamic stability of the H_2 complexes is reduced for **2a** and also **2b**. This suggests that the dihydrogen complexes gain in stability through conjugate base support,[12] which is not sufficiently provided by the ether molecule of the $[(3,5\text{-}(CF_3)_2C_6H_3)_4B]^-[H(OEt_2)]^+$ acid or the noncoordinating counterion BF_4^-.

The results obtained on the protonation behavior of compounds **1** can be summarized as follows.

(i) The protonation/deprotonation[13] equilibria (eq 2) are characterized by relatively high activation parameters. Positive $\Delta S^{\ddagger}$ values for these second-order reactions appear to be quite unusual.

(ii) The H/H exchange processes (eqs 3 and 4) are characterized by smaller activation parameters. $\Delta S^{\ddagger}$ values are negative.

(iii) The regioselective H/H exchange according to eq 3 requires an acid of medium strength. In this case, it is the fastest process and even operates in the absence of dihydrogen complexes.

(iv) The solvent polarity is presumed to have a more pronounced influence on the protonation (eq 2) than on the H/H exchange process (eq 3): decrease of the solvent polarity leads to retardation of the protonation of **1a** on the NMR time scale, while the hydrogen/hydrogen exchange is still operative.

(v) The KIE measured for the H/H exchange process of **1a** (eq 3) was found to be substantially higher than the KIE of the protonation reaction[14] (eq 2).

(vi) Conjugate base assistance is presumably required for both types of proton reactions (eqs 2 and 3).

The Intimate Mechanisms. The given observations can be interpreted within the framework of the protonation reaction (2), with the H/H exchanges according to eqs 3 and 4 as prekinetic steps for this process. Three different pathways, distinguished by the strength of the metal/hydrogen ligand(s) contact with or without participation of the conjugate base can be envisaged.

(A) The exchange proceeds via protolysis of the M–H bond.[15] This may or may not require support from the conjugate base.

$$L_nM\text{–}H \rightleftharpoons L_nM^- + H^+$$

$$B^- + L_nM\text{–}H \rightleftharpoons L_nM^- + HB$$

(B) The exchange occurs in strong binding contact to the metal center and once again (a) without or (b) with assistance from a conjugate base. This leads to transition states or intermediates of type (a) **Ia** or (b) **Ib** with a classical dihydride structure.

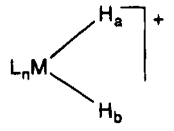

Ia

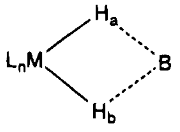

Ib

(C) In the course of the exchange process, the contact of the hydrogen ligands to the metal is loosened and dihydrogen complexes with either structure **IIa** or **IIb** are formed. Note that this situation is intermediate between cases A and B. **IIb** is distinguished from **IIa** by an additional interaction with a counterion.

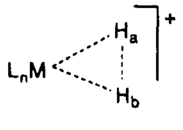

IIa

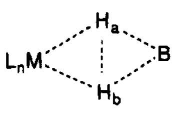

IIb

A transition state (TS) or intermediate of type **Ib** was suggested in the hydrogen/deuterium exchange of the negatively charged $HM(CO)_4L^-$ species (M = Cr, W).[1c] Structure **IIa** may be involved in the H/D exchange of

---

[10] Solution low-temperature ^2H T_1 times of the signals of CF_3COOD and of the D ligands of **1b** (in the absence of positional exchanges) are strongly different. For example, at −90 °C in toluene solution the T_1 value is <3 and 17 ms for CF_3COOD and **1b**, respectively. Because of positional exchanges the T_1 times are averaged, and this allows us to calculate according to ref 2a the corresponding exchange rates and activation parameters. The kinetic parameters of **5** in Table 2 were obtained by using this approach and the usual line-shape analysis.

[11] Brookhart, M.; Grant, B.; Volpe, A. F. *Organometallics* **1992**, *11*, 3920.

[12] Bianchini, C.; Mealli, C.; Peruzzini, M.; Zanobini, F. *J. Am. Chem. Soc.* **1992**, *114*, 5905.

[13] The p*Ka* value of ≅−1 (water scale) can be calculated from k_{-1} and k_1 values in Table 2 obtained for a CD_2Cl_2 solution of the nonclassical trihydride **2a**.

[14] Bullock, R. M. Isotope Effects in Reactions of Transition Metal Hydrides. In *Transition Metal Hydrides*; Dedieu, A., Ed.; VCH: Weinheim, Germany, 1992; pp 263–307.

[15] Kristjansdottir, S. S.; Norton, J. R. Acidity of Hydrido Transition Metal Complexes in Solution. In *Transition Metal Hydrides*; Dedieu, A., Ed.; VCH: Weinheim, Germany, 1992; pp 309–351.

$[IrH_2(DS(CH_2)_3SD)(PCy_3)_2][BF_4]$,[2c] which has a noncoordinating counterion.

The binding situation in the dihydrogen complexes **2** is likely to be intermediate between **IIa** and **IIb** and is presumably closer to structure **IIa**. In agreement with (iii)–(v), we propose structure **IIb** as the TS for the H/H exchanges of **1** according to eq 3. A reaction profile with **Ia,b** as intermediates or TS is deemed unlikely, since this would require initial attack of the protic substrate at the metal center. Finally, a transition state of type **IIa** can be eliminated, since it would contradict conditions (iii), (iv), and (vi).

Transition states of type **IIb** apparently dominate, if the strongly polarized O—H bond of the acid can interact favorably with sterically accessible hydridic M—H bonds. Note that a high ionic character of the metal–hydrogen bond has been established recently for the Re—D bond trans to the NO ligand in complexes **1** and **5**.[16] Compared to the hydridicity of the Re–D bond in $\mathbf{1^D}$, the Re—D bond polarity in $\mathbf{5^D}$ is somewhat reduced, which would provide an explanation for the observed slower D/D exchange rate of complex $\mathbf{5^D}$. The following order was found for complexes **1**–**5** (compound, k_1 in L/(mol s)): **5**, 0.92 × 10^2 (−60 °C, CH_2Cl_2) < $\mathbf{1b^D}$, 3.6 × 10^2 (−70 °C, $CH_2Cl_2/C_6H_5CH_3$) < $\mathbf{1a^D}$, 16.0 × 10^2 (−70 °C, $C_6H_5CH_3$) < $\mathbf{1c^D}$, 76.3 × 10^2 (−80 °C, CH_2Cl_2). The observed differences of the exchange rates within the series of nitrosyl-substituted compounds **1** are presumably due to steric influences of the phosphorus donors rather than due to electronic factors of these groups. Further investigations are required, however, to unambiguously establish the influence of the phosphorus ligands on the reaction rates.

A general scenario for the protonation reactions of metal hydride complexes which involves the transition state **IIb** as a precursor to nonclassical dihydrogen complexes is shown in eq 5. The reaction sequence may be actually initiated by a hydrogen-bonding contact of the acid proton and the hydridic M—H bond, which subsequently adopts the more compact structure **IIb** (eq 5). A fast and (reversible) base dissociation step from the base-supported structure **IIb** would then complete the reaction and give the nonclassical H_2 complex.

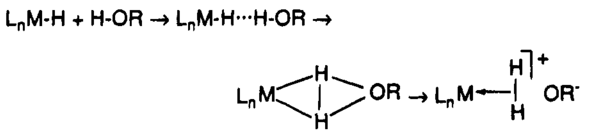

$$L_nM\text{-}H + H\text{-}OR \rightarrow L_nM\text{-}H\cdots H\text{-}OR \rightarrow L_nM\langle H, H\rangle OR \rightarrow [L_nM\leftarrow (H\text{-}H)]^+\ OR^- \qquad (5)$$

The present work provides kinetic evidence for the different types of $M—H^{\delta-}\cdots H^{\delta+}—X$ interactions shown in eq 5.[2a,15] The suggested hydrogen-bonding contact of the acid proton and the metal hydride exchanges may appear at first glance quite speculative but have some support from a low-temperature neutron diffraction study of *cis*-$[IrH(OH)(PMe_3)_4]^+$, which reveals a quite short intramolecular interaction between the $Ir—H^{\delta-}$ and $OH^{\delta+}$ groups.[17]

Metal hydride/acidic substrate contact pairs could also play a role in the reduction of aldehydes or ketones to alcohols.[18] Hence, we examined the reduction of benzaldehyde to the benzyl alcohol complex by **1a** in the presence of CF_3COOH at −80 °C in CD_2Cl_2. After 6 h, a conversion of 45% was observed in this reaction, monitored by ^1H and ^{13}C NMR spectroscopy, which contained an approximate 1/1/1 ratio of **1a**, CF_3COOH, and benzaldehyde initially. At higher temperatures, the benzyl alcohol complex $[ReH(CO)(NO)(PiPr_3)_2(C_6H_5CH_2OH)]^+$ could be identified by NMR spectroscopy.[19] Elimination of the benzyl alcohol molecule from this species finally completed the reaction sequence.

EHT Calculations. EHT model calculations for complex 2 have been carried out to provide a better understanding of the site preference for the binding of the H_2 ligand to a square-pyramidal $[ReH(CO)(NO)L_2]^+$ moiety. To simplify the calculations and to facilitate the analysis, we have chosen an idealized pseudooctahedral fragment with L = PH_3. Even with these restrictions, it became apparent that the two isomers **8a,b** have different potentials for H_2 binding.

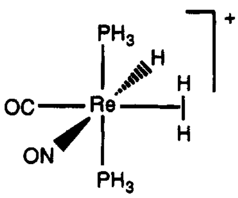

8a

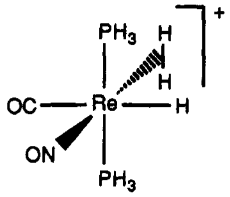

8b

For the preference of **8a** over **8b**, the energy 2.2 kcal/mol was calculated, which supports the proposed geometry for the prevailing isomers of **2a**–**c** with the H_2 ligand trans to the CO group (structure **8a**). The barriers of rotation for the dihydrogen ligand in **8a,b** were estimated from calculations of the ∥ and ⊥ rotamers of **8a,b** (axis ∥ or ⊥ to the Re—P axis). Within the given restricted geometric model, we found 3.4 kcal/mol for **8a** and 0.1 kcal/mol for **8b** ($\mathbf{8a}_{\parallel}$ and $\mathbf{8b}_{\perp}$ energetically favored).

The different binding energetics in the isomers **8a,b** are quite easily explained. The H_2 ligand represents a single-faced π acceptor (comparable to ethylene), and its binding to a transition-metal center consists of a σ-donor and a π-acceptor bond.[2a,20] Since the π-bonding capability of a transition-metal fragment is reduced in a position trans to the strong π acceptor NO, the H_2 ligand cannot find a reasonable π-type interaction in this location. Hence, structure **8a**, with the weaker CO π-acceptor ligand in the trans position, becomes energetically more favorable. The barrier of rotation around the Re—(H_2) axis is therefore essentially nonexistent in **8b** and is also higher in **8a**. As another consequence of the reduced π donation from the metal to the H_2 group in **8b**, the H_2 moiety becomes more electrophilic than

---

[16] Nietlispach, D.; Bakhmutov, V. I.; Berke, H. *J. Am. Chem. Soc.* **1993**, *115*, 9191.

[17] Stevens, R. C.; Bau, R.; Milstein, D.; Blum, O.; Koetzle, T. F. *J. Chem. Soc. Dalton. Trans.* **1990**, 1429.

[18] Song, J.-S.; Szalda, D. J.; Bullock, R. M.; Lawrie, C. J. C.; Rodkin, M. A.; Norton, J. R. *Angew. Chem.* **1992**, *104*, 1280. Van der Zeijden, A. A. H.; Bosch, H. W.; Berke, H. *Organometallics* **1992**, *11*, 2051. Kundel, P.; Berke, H. *J. Organomet. Chem.* **1987**, *335*, 353.

[19] ^1H NMR at −80 °C in CD_2Cl_2: δ 8.61 (broadened s, 1H, OH), 7.3 (broadened s, 5H, C_6H_5), 4.92 (broadened s, 2H, CH_2), 3.8 (tr, $^2J_{HP}$ = 26 Hz, 1H, ReH), 2.4 (broadened m, CH), 1.25 (broadened m, CH_3). $^{13}C\{^1H\}$ NMR: δ 74.2 (s, CH_2), 128.2, 128.3, 128.4 (s, C_6H_5), 210.0 (broadened tr, $^2J_{CP} \cong$ 8 Hz, CO), 24.5 (broadened m, CH), 19.0 (broadened m, CH_3). $^{31}P\{^1H\}$ NMR: δ 41.5 (s, broadened).

[20] Burdett, J. K.; Eisenstein, O.; Jackson, S. A. *Transition Metal Dihydrogen Complexes*: Theoretical Studies In *Transition Metal Hydrides*; Dedieu, A., Ed.; VCH: Weinheim, Germany, 1992; pp 149–184.

in **8a**. For this reason, **8b** might show an enhanced tendency to associate with an acid anion, comparable to the proposed transition state **IIb**. We have tried to model the anion assistance, using the symmetrical pseudooctahedral model compounds **9** and **10**, and to trace the trans π-acceptor ligand influence in our calculations.

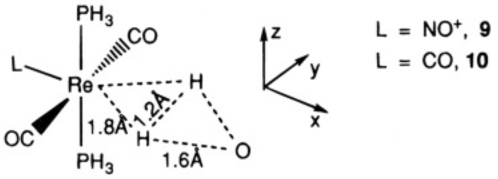

The $[Re(CO)_2H(NO)(PH_3)_2]^+$ fragment of **9** relates to complexes **1**; H^+ and O^{2-} represent the acid. A reasonable nonoptimized structure, however, of such an interaction is given in the sketch of **9**. The model calculations reveal quite feasible features for the orbital interactions in **9**, i.e. a reasonable HOMO/LUMO gap (~2.5 eV), and also show crucial participation of the oxygen orbitals in the binding of the H_2 unit to the metal center. The orbital interactions of the $Re(H_2)O$ unit for this transition-state model are built up mainly by d_{xy} and σ-type functions on rhenium, by the two s_H orbitals or hydrogen, and by s, p_x, and p_y orbitals of the oxygen atom. It deserves special mention, however, that the s orbital participation of the O atom is of minor relevance. The fragment has to accommodate four pairs of electrons, one pair originating from d_{xy}, one from the H atoms, and two from p_x and p_y from oxygen. One σ- and one π-type three-centered orbital interaction, represented schematically, have to be filled up to their "nonbonding" level:

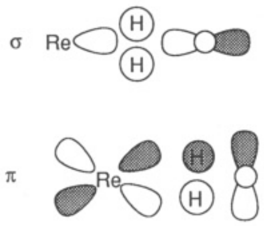

The two nonbonding orbitals (not shown) are found in a delicate energetic balance; i.e., a weak H—H contact is necessary to keep the σ_{H_2} (for σ) and $\sigma^*_{H_2}$ (for π) orbitals in energetic vicinity to the orbitals of both the Re metal center and oxygen, since relevant interaction with both sides of the H,H axis can otherwise not be anticipated. It should be noted, however, that the interactions of the model conjugate base, the O^{2-} anion, are energetically balanced, as evidenced by the small positive total overlap population (+0.0001) between the H atoms and O^{2-}.

In a further EHT calculation, the influence of the stronger NO π acceptor on the TS structure **IIb** was probed. With the same geometry used as in the calculation of **9**, the H_2/O^{2-} total overlap population of −0.0016 in **10** now indicated a weak electronic repulsion between the $[Re(H_2)(CO)_3(PH_3)_2]^{2+}$ fragment and the O^{2-} ion. This suggests that the π-accepting power of the trans NO group is essential for the stabilization of an oxoanion-supported H_2 ligand moiety.

These calculations support the idea that NO groups destabilize nonclassical H_2 ligands in trans positions on the other hand, they also indicate that the NO ligand promotes the formation of oxoanion-assisted H_2 units with a **IIb**-type structure. Further experimental work is required, however, to establish **IIb** as a TS or intermediate in protonation reactions and is currently being pursued in our laboratories.

Experimental Section

EHT calculations[21] were performed using the CACAO program package.[22] The parameters for Re were as follows: 5d, $H_{ii} = -12.1$ eV, $\zeta_1 = 3.853$; $\zeta_2 = 1.505$, $c^1 = 0.6211$, $c^2 = 0.5796$; 6s, $H_{ii} = -10.1$ eV, $\zeta = 1.776$; 6p, $H_{ii} = -6.86$ eV, $\zeta = 1.817$. Those for the other atoms were the standard parameters of CACAO. The following distances (Å) were used in the computational procedures: Re—CO, 1.92; Re—NO, 1.80; Re—PH_3, 2.43; Re—(H_2), 1.72; C—O, 1.08; N—O, 1.18; P—H, 1.40.

All manipulations were performed by standard Schlenk techniques under a dry nitrogen atmosphere. Solvents (CH_2Cl_2, CD_2Cl_2, toluene-d_8, and toluene) were dried by conventional procedures and freshly distilled before use. IR spectra were recorded on a Biorad FTS45 instrument, and mass spectra were obtained on a Finnigan MAT 8240 spectrometer. Variable-temperature ^1H, ^2H, ^{31}P, and ^{31}C NMR spectra were obtained on Varian Gemini-300 (300 MHz for ^1H) and Bruker VP-200SY (200 MHz for ^1H) spectrometers. ^1H NMR saturation transfer experiments were performed by standard techniques of the spectrometer. The inversion-recovery method (180°−τ−90°) was used to determine ^2H T_1 relaxation times. The calculations of the relaxation times were performed with the nonlinear three-parameter fitting routine of the Gemini-300 spectrometer.

Compounds **1** $(ReH_2(CO)(NO)(PR_3)_2)$ were prepared as described in the literature.[4] The D isotopomers $ReD_2(CO)(NO)(PR_3)_2$ were obtained from the corresponding ReH_2 complexes by H/D exchange at 50 °C with CD_3OD in toluene. The H/D exchanges were monitored by ^1H NMR spectroscopy, and the solvent mixtures were evaporated *in vacuo* after completion of the reaction. The ^2H NMR data of these complexes and details of their preparation can be found in ref 1d.

^{1}H NMR Investigations of the $[Re(H_2)H(CO)(NO)L_2]^+$ Complexes 2. The CD_2Cl_2 solutions of complexes **2** were obtained by acidification of solutions of **1** with variable ratios (for details see text) of the acids CF_3COOH and $HBF_4{\cdot}2Et_2O$ at low temperatures (−120 to −70 °C).

2a: for NMR data see ref 5.

2b: ^1H NMR (CD_2Cl_2, 173 K, 200 MHz) δ 4.50 (CH), 1.29 (CH_3), −1.7 ($Re(H_2)$), −2.18 (t, $^2J_{PH} = 26$ Hz, Re—H); $^{31}P\{^1H\}$ NMR: δ 99.5.

2c: ^1H NMR (CD_2Cl_2, 170 K, 200 MHz) δ 1.63 (CH_3), −1.6 to −1.7 ($Re(H_2)$), −1.94 (t, $^2J_{PH} = 27.5$ Hz, Re—H); $^{31}P\{^1H\}$ NMR δ −39.2.

Synthesis of $ReH(CO)(NO)L_2(OC(O)CF_3)$ (3a−c). A solution of **1a,b** (0.45 mmol) in 5 mL of toluene was reacted at room temperature with 1.2 equiv of CF_3COOH (0.54 mmol). An immediate evolution of H_2 occurred, and after 2 h the solution was evaporated to dryness. The oily residue was extracted with ether and filtered through Celite. Recrystallization from hexane/ether at −30 °C gave yellow crystals of **3a,b**. Yield: 83%, **3a**; 79%, **3b**.

For **3c**, a solution of **1c** in CH_2Cl_2 was treated with CF_3COOH at −40 °C. The oily residue was extracted with hexane. Recrystallization from hexane yielded 80% of **3c**.

3a: IR (ether) $\nu(C{\equiv}O)$ 1957 (vs), $\nu(N{\equiv}O)$ 1724 (vs), ν(Re—H) 1893 (w), ν(OCO) 1704, 1683 (w) cm^{-1}; MS (EI) *m/e* 678 ($M^+ - H$), 651 ($M^+ - CO$), 608 ($M^+ - CO - C_3H_9$), 565 ($M^+ - CO - 2C_3H_9$), 565 ($M^+ - H - CO_2CF_3$); ^{31}P NMR (C_6D_6) δ 41.4; ^1H NMR (C_6D_6) δ 2.39 (t, $^2J_{PH} = 26.5$ Hz, 1H, Re—H), 2.15 (m,

---

[21] Hoffmann, R.; Limpscomb, W. N. *J. Chem. Phys.* **1962**, *36*, 2179.

[22] Mealli, C.; Proserpion, D. M. *J. Chem. Educ.* **1990**, *67*, 399.

6H, CH), 1.08 (m, 36H, CH_3); ^{13}C NMR (C_6D_6) δ 210.6 (t, $^2J_{PC}$ = 6.4 Hz, CO), 161.8 (q, $^2J_{FC}$ = 36.9 Hz, OC(O)), 115.6 (q, J_{FC} = 290.5 Hz, CF_3), 25.6 ("t", J_{PC} = 25 Hz, PC), 19.0, 18.9 (s, CH_3), $^2J_{H^{13}CO}$ = 8.9 Hz. Anal. Calcd for $C_{21}H_{43}F_3NO_4P_2Re$: C, 37.16; H, 6.37; N, 2.06. Found: C, 36.92; H, 6.13; N, 2.36.

3b: IR (hexane): $\nu(C\equiv O)$ 2019 (vs), 1996 (s), $\nu(N\equiv O)$ 1730 (s), ν(Re—H) 1855 (w), ν(OCO) 1702 (w) cm^{-1}; MS (EI) *m/e* 774 (M^+ − H), 747 (M^+ − H − CO), 661 (M^+ − H − CO − CO_2CF_3); ^{31}P NMR (C_6D_6) δ 113.6; ^1H NMR (C_6D_6) δ 4.73 (m, J_{HH} = 6.1 Hz, 6H, CH), 3.07 (t, $^2J_{PH}$ = 30.9 Hz, 1H, Re—H), 1.20 (d, J_{HH} = 6.1 Hz, 18H, CH_3), 1.19 (d, J_{HH} = 6.1 Hz, 18H, CH_3); ^{13}C NMR (C_6D_6) δ 201.8 (t, $^2J_{PC}$ = 10.2 Hz, CO), 162.6 (q, $^2J_{FC}$ = 37.2 Hz, OC(O)), 115.6 (q, J_{FC} = 289.7 Hz, CF_3), 71.4 (s, CH), 23.9 (s, CH_3), $^2J_{H^{13}CO}$ = 10.2 Hz. Anal. Calcd for $C_{21}H_{43}F_3NO_{10}P_2Re$: C, 32.56; H, 5.57; N, 1.81. Found: C, 32.88; H, 5.39; N, 1.79.

3c: IR (hexane): $\nu(C\equiv O)$ 1972 (vs), $\nu(N\equiv O)$ 1723 (s) ν (Re—H) 1818 (w), ν(OCO) 1684 (w) cm^{-1}; MS (EI) *m/e* 510 (M^+ − H), 483 (M^+ − H − CO), 480 (M^+ − H − NO), 452 (M^+ − H − NO = CO); ^{31}P NMR (CD_2Cl_2, −40 °C) δ −24.1; ^1H NMR (CD_2Cl_2, −30 °C) δ 2.08 (t, $^2J_{PH}$ = 27.0 Hz, 1H, Re—H), 1.62 ("t" J_{PH} = 8.6 Hz, 18H, CH_3); ^{13}C NMR (CD_2Cl_2, −30 °C) δ 207.9 (t, $^2J_{PC}$ = 6.3 Hz, CO), 161.4 (q, $^2J_{FC}$ = 36.0 Hz, OC(O)), 114.9 (q, J_{FC} = 290.1 Hz, CF_3), 17.0 ("t", J_{PC} = 35.3 Hz, CH_3), $^2J_{H^{13}CO}$ = 9.9 Hz. Anal. Calcd for $C_9H_{19}F_3NO_4P_2Re$: C, 21.18; H, 3.75; N, 2.74. Found: C, 21.46; H, 4.02; N, 2.50.

Synthesis of $Re(CO)(NO)L_2(OC(O)CF_3)_2$ (4a–c). A solution of **1** (0.45 mmol) in 5 mL of toluene was treated at room temperature with an excess of CF_3COOH. After complete evolution of H_2 (1 h) the solution was evaporated to dryness. The oily residue was extracted with CH_2Cl_2 and filtered through Celite. Recrystallization from hexane/CH_2Cl_2 at −30 °C gave yellow crystals of **4**. Yield: 90%, **4a**; 87%, **4b**; 85%, **4c**.

4a: IR (ether): $\nu(C\equiv O)$ 2001 (vs), $\nu(N\equiv O)$ 1755 (vs), ν(OCO) 1714 (w), 1702 (w) cm^{-1}; MS (EI) *m/e* 792 (M^+), 679 (M^+ − CO_2CF_3), 651 (M^+ − CO_2CF_3 − CO); ^{31}P NMR (C_6D_6) δ 27.3; ^1H NMR (C_6D_6) δ 2.22 (m, 6H, CH), 1.08 (m, CH_3, 36H); ^{13}C NMR (C_6D_6) δ 205.5 (t, $^2J_{PC}$ = 6.3 Hz, CO), 161.2 (q, $^2J_{FC}$ = 38.3 Hz, OC(O)), 161.0 (q, $^2J_{FC}$ = 37.2 Hz, OC(O)), 116.4 (q, J_{FC} = 290.3 Hz, CF_3), 116.0 (q, J_{FC} = 289.6 Hz, CF_3), 19.2, 19.1 (s, CH_3). Anal. Calcd for $C_{23}H_{42}F_6NO_6P_2Re$: C, 34.89; H, 5.35; N, 1.77. Found: C, 35.07; H, 5.08; N, 1.86.

4b: IR (hexane) $\nu(C\equiv O)$ 2051 (s), 2033 (vs), $\nu(N\equiv O)$ 1785 (vs), 1766 (vs) ν(OCO) 1720 (s), 1705 (s) cm^{-1}; MS (EI) *m/e* 887 (M^+), 859 (M^+ − CO), 829 (M^+ − CO − NO), 774 (M^+ − CO_2CF_3), 746 (M^+ − CO_2CF_3 − CO); ^{31}P NMR (C_6D_6) δ 100.6; ^1H NMR (C_6D_6) δ 4.65 (m, J_{HH} = 6.1 Hz, 6H, CH), 1.17 (d, J_{HH} = 6.1 Hz, 18H, CH_3), 1.16 (d, J_{HH} = 6.1 Hz, 18H, CH_3); ^{13}C NMR (C_6D_6) δ 197.1 (t, $^2J_{PC}$ = 10.7 Hz, CO), 163.4 (q, $^2J_{CF}$ = 38.1 Hz, OC(O)), 162.4 (q, $^2J_{CF}$ = 38.0 Hz, OC(O)), 115.9 (q, J_{FC} = 288.5 Hz, CF_3), 115.8 (q, J_{FC} 288.3 Hz, CF_3), 72.4 ("t", J_{PC} = 6.2 Hz, PC), 23.8, 23.7 (s, CH_3). Anal. Calcd for $C_{23}H_{42}F_6NO_{12}P_2Re$: C, 31.12; H, 4.77; N, 1.58. Found: C, 31.41; H, 4.98; N, 1.71.

4c: IR (ether): $\nu(C\equiv O)$ 2009 (s), $\nu(N\equiv O)$ 1763 (vs), ν(OCO) 1719 (w), 1704 (w) cm^{-1}; MS (EI) *m/e* 623 (M^+), 595 (M^+ − CO), 510 (M^+ − CO_2CF_3), 482 (M^+ − CO_2CF_3 − CO); ^{31}P NMR (CD_2Cl_2) δ −15.2; ^1H NMR (CD_2Cl_2) δ 1.60 ("t", J_{PH} = 8.6 Hz, 18H, CH_3); ^{13}C NMR (CD_2Cl_2) δ 201.5 (t, $^2J_{PC}$ = 6.0 Hz, CO), 163.8 (q, $^2J_{FC}$ = 38.6 Hz, OC(O)), 162.9 (q, $^2J_{FC}$ = 39.2 Hz, OC(O)), 115.6 (q, J_{FC} = 288.1 Hz, CF_3), 115.4 (q, J_{FC} = 287.9 Hz, CF_3), 13.5 ("t", J_{PC} = 33.9 Hz, CH_3). Anal. Calcd for $C_{11}H_{18}F_6NO_6P_2Re$: C, 21.23; H, 2.92; N, 2.25. Found: C, 21.36; H, 3.09; N, 2.38.

Crystal Structure Determination of 3c. A crystal of $Re(H)(OOCCF_3)(CO)(NO)(PMe_3)_2$ (**3c**) was mounted in air on a glass fiber using 5 min epoxy resin. The unit cell was determined and refined from 24 equivalent reflections with $2\theta \geq$ 26–28° obtained on a Siemens R3/m four-circle diffractometer. Intensity data were collected at −60 °C and corrected for Lorentz and polarization effects. Three check reflections, monitored periodically for crystal decomposition or movement, showed no significant variations in these standards, and therefore no correction was applied. The structure was solved by direct methods, from which the positions of the Re and P atoms were located. The other atoms were found in subsequent Fourier maps. Anisotropic refinement was applied to all non-hydrogen atoms.

Table 3. Data Collection and Processing Parameters of 3c

formula	$C_9H_{19}F_3NO_4P_2Re$
mol wt	510.4
color and habit	yellow prism
space group	$P2_1/n$ (No. 14)
a, Å	10.290(2)
b, Å	11.454(3)
c, Å	15.232(4)
β, deg	101.01(2)
V, Å^3	1762.2(7)
Z	4
ϱ_{calcd}, g cm^{-3}	1.924
radiation; λ, Å	graphite monochromator, Mo Kα; 0.170 73
temp. °C	−60
abs coeff, cm^{-1}	72.04
cryst size, mm	0.25 × 0.25 × 0.20
scan type	$\omega-2\theta$
scan speed, deg/min	variable; 2.02−14.65
scan width, deg	1.80
collecn range	$h,k,\pm l$
2θ range, deg	4−54
no. of unique data	4126
no. of reflns obsd	3319 ($F \geq 4\sigma(F)$)
no. of variables	181
weigthing scheme	$w^{-1} = \sigma^2(F) + 0.0050F^2$
R	0.043
R_w	0.079
residual extrema in final diff map, e/Å^3	+1.04, −1.46

Table 4. Atomic Coordinates (×10^4) and Equivalent Isotropic Displacement Coefficients (Å^2 × 10^3) for 3c

	x	*y*	*z*	*U*(eq)[a]
Re(1)	4586(1)	2148(1)	1254(1)	42(1)
P(1)	6630(3)	3215(2)	1372(2)	58(1)
P(2)	2966(2)	610(2)	1292(2)	45(1)
O(1)	4096(11)	2228(8)	−772(6)	108(1)
O(2)	2874(9)	4243(6)	1277(5)	87(1)
O(3)	4616(11)	3270(7)	3323(5)	110(1)
O(4)	5192(6)	1707(5)	2643(4)	48(1)
F(1)	6638(8)	1364(9)	4365(5)	134(1)
F(2)	4809(10)	642(7)	4179(5)	139(1)
F(3)	5182(11)	2229(7)	4871(5)	130(1)
N(1)	3539(7)	3400(6)	1339(4)	50(1)
C(1)	4271(11)	2211(7)	−23(6)	63(1)
C(2)	5003(9)	2315(7)	3303(6)	53(1)
C(3)	5357(9)	1643(8)	4182(6)	59(1)
C(11)	6791(13)	4513(10)	2031(10)	138(1)
C(12)	7943(12)	3597(11)	300(8)	119(1)
C(13)	8091(12)	2439(11)	1824(11)	124(1)
C(21)	2140(10)	5(8)	226(6)	68(1)
C(22)	3626(9)	−649(7)	1918(7)	62(1)
C(23)	1620(8)	1051(8)	1823(6)	56(1)
H(1)	5524(16)	1090(15)	941(12)	50(3)

[a] Equivalent isotropic *U*, defined as one-third of the trace of the orthogonalized $\mathbf{U}_{ij}$ tensor.

The H atoms of the PMe_3 ligands were generated geometrically (C—H bond fixed at 0.96 Å), and a temperature factor of *U* = 0.08 Å^2 was assigned to all H atoms. The hydride atom H(1) was found in the difference Fourier map and refined isotropically. The DIFABS method[23] was used for the absorption correction at the stage of the isotropic approximation. Computations were performed with the SHELXTL PLUS program package[24] on a VAX-Station 3100. Details of the crystal parameters, data collection, and structure refinement

---

(23) Walker, N.; Stuart, D. *Acta Crystallorg.* **1983**, *A39*, 158.

are given in Table 3. Positional parameters and equivalent isotropic thermal parameters can be found in Table 4. Additional information is available as supplementary material.

Acknowledgment. We thank the Swiss National Science Foundation for financial support. Thanks are also due to Dr. D. Nietlispach for the synthesis of *cis*-$ReD(CO)(PMe_3)_4$.

Supplementary Material Available: Tables giving additional details of the X-ray structure determination, additional bond lengths and angles, anisotropic thermal parameters, and hydrogen atom coordinates for **3c** (7 pages). Ordering information is given on any current masthead page.

OM930889A

---

(24) Sheldrick, G. M. *Crystallographic Computing 3: Data Collection, Structure Determination, Proteins and Databases*; Oxford University Press: New York, 1985; p 175.